Simulation of Metal Vapor Breakdown after Interrupting a Vacuum Arc

Zhenxing Wang, Yingsan Geng, Zhiyuan Liu
State Key Laboratory of Electrical Insulation and Power Equipment, Xi'an Jiaotong University, Xi'an 710049, China

***Abstract*- A breakdown after interrupting a vacuum arc current indicates the interruption limit of a vacuum circuit breaker (VCB). The objective of this paper is to study breakdowns in copper vapor at a density of interruption limit employing Particle in Cell-Monte Carlo Collision (PIC-MCC) method. A model with one dimension in physical space and three dimensions in velocity space was developed with a gap length of 10mm between the contacts. The model took into account ionization, excitation, elastic collision and secondary emission. We obtained the boundary of instantaneous breakdown region of a VCB through the simulation. The results show that a higher neutral metal vapor density can accelerate the electron avalanche process but the influence was limited when the density exceeded a certain level. Moreover, a higher voltage can also accelerate the avalanche process.**

I. INTRODUCTION

Dielectric recovery processes after vacuum arc interruptions have been extensively studied in order to find out the interruption limit of a vacuum circuit breaker (VCB) [1-3]. After current zero, a number of residual particles including electrons, ions, droplets and neutral metal vapor remain in the switching gap between contacts. Moreover, the number of particles decays under the influence of a transient recovery voltage (TRV) until the switching gap is restored to a vacuum state.

A dielectric recovery process can be divided into three stages according to the species of the particles which dominate the evolution of the process[4]. At the first stage, also the initial stage after current zero, quasi-neutral plasma which is composed of ions and electrons remains in a contact gap with background neutral metal vapor. With the effect of a TRV, a sheath forms in front of the post-arc cathode and develops toward the post-arc anode. At this stage, electrons, ions and the TRV applied upon the sheath plays an important role in the interruption capacity of a VCB. After the sheath development, a large amount of metal vapor may still remain in the switching gap because of the emission of the hot contact surface especially after high-current interruptions. The hot surface emits electrons to the switching gap due to thermionic emission mechanism. The electrons are accelerated by the TRV, and collided with the metal vapor which may produce secondary electrons and ions. Thus, a breakdown may occur on account of the charge carrier multiplication. In addition, the secondary species bombarding the contact surface may lead to a further emission of the hot surface. At this stage, it is assumed that the Townsend mechanism is the primary cause for the breakdowns. After the density of the metal vapor dropping to a certain level, the vacuum interrupter can withstand its full design voltage, and the recovery process is completed. Although residual plasma has great impact on the recovery at the initial stage, metal vapor will play a decisive role in connection with the interruption limit of a VCB because the duration of sheath development is quite shorter than that of metal vapor which lasts about several milliseconds.

Many researchers have developed various numeric models to unveil the physical process after current interruptions [5-7]. Andrews and Varey[8] provided a continuous transition model which was deduced from Child's law and the ion matrix model to describe sheath development. Thereafter, the model has predicted sheath development after current zero successfully. Moreover, Sarrailh et al.[9] have used direct simulation Monte-Carlo (DSMC) method to calculate sheath development in order to obtain the detail description of the physical process. However, the researchers mainly focused on sheath development rather than breakdowns in background metal vapor which determines the interruption capacity of a VCB.

The objective of this paper is to simulate breakdowns in copper vapor at a density of interruption limit. We adopted Particle in Cell-Monte Carlo Collisions (PIC-MCC) method considering the physical processes including ionization, excitation, elastic collision and secondary emission. A model with one dimension in physical space and three dimensions in velocity space was developed. We simulated the evolution of electron energy distribution function (EEDF) during the breakdown processes. We also evaluated the influence of neutral metal vapor density on the evolution of the breakdown. Moreover, we obtained the boundary of instantaneous breakdown region of a VCB.

This work was supported by the National Natural Science Foundation of China under Project No. 51177122.

978-1-4673-1265-3/12/$31.00 ©2012 IEEE

II. SIMULATION

A. PIC-MCC Method

Particle-in-Cell (PIC) is a kind of simulation method for studying plasma physics based on the evolution of plasma distribution function in phase space[10]. Compared with a fluid model of plasma, a PIC model is able to solve the Vlasov function without assuming a distribution function in the velocity space. Consequently, we can obtain the behaviors of plasma under a non-equilibrium condition due to a small amount of particles in plasma with a low temperature. Generally, the non-equilibrium condition always occurs after vacuum arc interruptions because particles generating in an arcing period may be dissipated or/and absorbed rapidly in a dielectric recovery period.

PIC, however, may invalid when we have to consider the effect of a short-range collision when the Coulomb interaction dominates the collision. In order to solve this problem, researchers introduced Monte Carlo collision method to simulate the short-range collisions. Thus, we can use PIC-MCC method to model the breakdown after interruption which involves ionization, excitation and secondary emission.

First of all, we define macro-particles which represent a number of real particles in plasma. Then the charge of the macro-particles is assigned to the simulation grid so that we can obtain the distribution of charges in the simulation region. According to the distribution, the electromagnetic force is solved by the Maxwell equations. Next the motion of a particle can be calculated by classic or relative motion equations. MCC method is used to simulate collisions such as ionization, excitation and the elastic scattering collision. The possibility of the collisions can be described as:

$$P = 1 - \exp[-v\Delta t\sigma(\varepsilon)n(x)] \quad (1)$$

where P is the possibility of the collisions, v is the velocity of the particles, Δt is the time step of the simulation, σ is the total cross sections of all kind of collisions, ε is the energy of the particles and n is the background vapor density. Generally, the null collision arithmetic is adopted in calculating the collisions in order to achieve a higher efficiency[11].

B. The Numerical Model

With the aid of PIC-MCC method, we can simulate the breakdown process after interrupting a vacuum arc. A model with one dimension in physical space and three dimensions in velocity space (1d3v) was developed with a gap length of 10mm between the contacts. Moreover, a negative direct voltage was applied upon the contacts.

Fig. 1 shows the schematic diagram of the model. As we simulated the beginning of a breakdown, only the three species Cu neutral, Cu+ ions and electrons are taken into accounted. We assumed the background neutral metal vapor at a temperature of 0.2eV[2]. The density of metal vapor varied from 10^{21} m^{-3} to 10^{23} m^{-3} which are considered to be the instantaneous breakdown region of a VCB in a high current interruption. Moreover, the density of metal vapor remained constant during the simulation. We impressed a negative TRV across a contact gap from 1 kV to 10 kV. We considered secondary emission due to the ions impact on the contact surfaces. The secondary emission rate was taken from a reference[12]. The particles were absorbed by the boundaries when they reached the boundaries (contact surfaces) of the model. Following collisions are relevant and have been taken into account:

$$Cu + e^- \rightarrow Cu^+ + 2e^- \quad (2)$$

$$Cu + e^- \rightarrow Cu^* + 2e^- \quad (3)$$

$$e^- + Cu \rightarrow e^- + Cu \quad (4)$$

In order to obtain the boundary of instantaneous breakdown region, we attempted a large range of electric voltages to probe the breakdown voltage of metal vapor densities from 0.5×10^{21} m^{-3} to 10^{21} m^{-3}. The criterion of a breakdown is the number of electrons after a DC voltage is applied. If the number of electrons increases smoothly without the multiplication, and keeps constant after growth process, we consider the voltage cannot induce a breakdown at this metal vapor density.

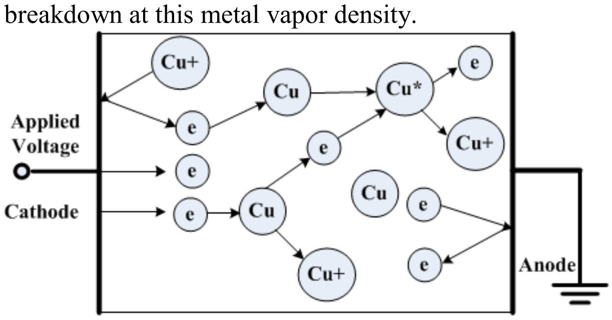

Fig. 1. Schematic diagram of the one-dimensional simulation modeling the breakdown after current interruptions.

RESULTS AND DISCUSSION

Fig. 2 shows the ion density profile at 0.2ns, 0.7ns and 1.4ns after a voltage applied upon the contact gap. The neutral metal vapor density was 10^{22} m^{-3}. The applied voltage was 5kV. The curves were fitted on the original data. The ion density increased with the time after the voltage applied. Moreover, the ion density did not increase homogeneous along the contact gap but initialized nearby the cathode surface. However, the ion density nearby the anode surface was higher than that nearby the cathode surface when the ion was filled with the gap. It is suggested that electrons which emit from the collision between incident electrons and neutral metal vapor dominant a breakdown process after an avalanche begins.

Fig. 3 shows the electron energy distribution function at 0.2ns, 0.7ns and 1.4ns after a voltage applied upon the contact gap, respectively. The neutral metal vapor density was 10^{22} m^{-3}. The applied voltage was 5kV. At the moment of 0.2ns after the voltage applied, the electrons were mainly composed by incident electrons so the majority of the electrons possessed energy less than 2eV. However, the electrons with a high energy emerged after the electron avalanche tunnel formed.

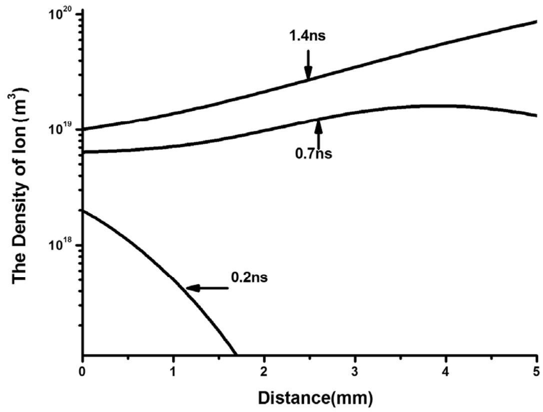

Fig. 2. The profiles of ion density at the moment 0.2ns, 0.7ns and 1.4ns. Metal vapor density: 10^{22} m^{-3}; Voltage: 5kV.The curves were fitted on the original data.

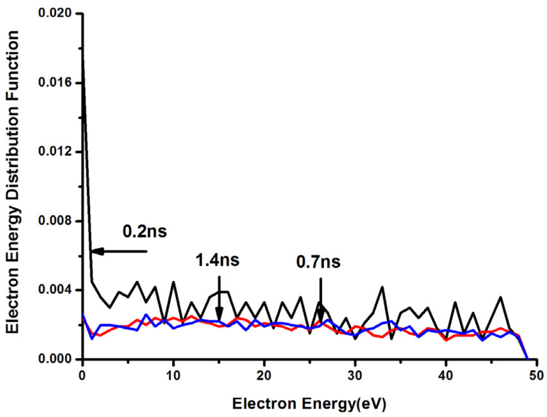

Fig. 3. The electron energy distribution functions at the moment 0.2ns, 0.7ns and 1.4ns. Metal vapor density: 10^{22} m^{-3}; Voltage: 5kV.

Fig. 4 shows the ion density profile at 0.7ns and 1.4ns after a voltage applied upon the contact gap. The neutral metal vapor density was 10^{23} m^{-3}. The applied voltage was 5kV. Although the ions initialized nearby the cathode, the number of the ions increased more rapidly compared with Fig. 2. At the moment of 1.4ns, the peak value of ion density exceeded 10^{30} m^{-3} for metal vapor with a density of 10^{23} m^{-3}. However, the peak value of ion density for metal vapor density 10^{22} m^{-3} was lower than that for 10^{20} m^{-3} at the same moment. It is clear that the ion density increased as the neutral metal vapor went up. It is also suggested that the neutral metal vapor density plays an important role in the breakdown process. A higher metal vapor density leads to a breakdown easier.

Fig. 5 shows the electron energy distribution function at 0.2ns, 0.7ns and 1.4ns after a voltage applied upon the contact gap. The neutral metal vapor density was 10^{23} m^{-3}. The applied voltage was 5kV. At the moment of 0.2ns after the voltage applied, the electron energy was less than 20eV which is much higher than the electron energy 2eV for the case of metal vapor density 10^{22} m^{-3} shown in Fig. 3. Moreover, the proportion of high-energy electrons after the electron avalanche tunnel formed was higher than that of metal vapor density 10^{22} m^{-3} shown in Fig. 3. And the neutral metal vapor density had a significant influence on the electron energy. The electron energy has a direct impact on a breakdown process. It is obvious that an electron with higher energy leads to a breakdown easier. Furthermore, the multiplication of ion is also related to the electron energy.

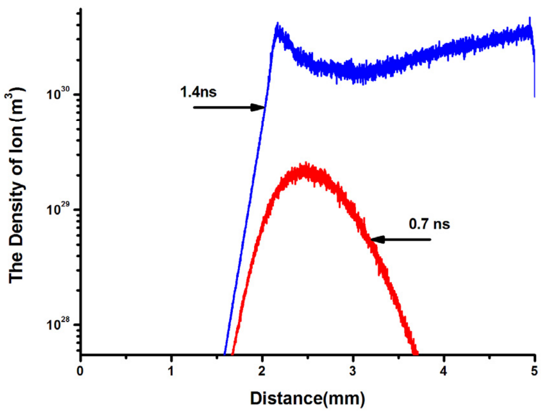

Fig. 4. The profiles of ion density at the moment 0.7ns and 1.4ns. Metal vapor density: 10^{23} m^{-3}; Voltage: 5kV.

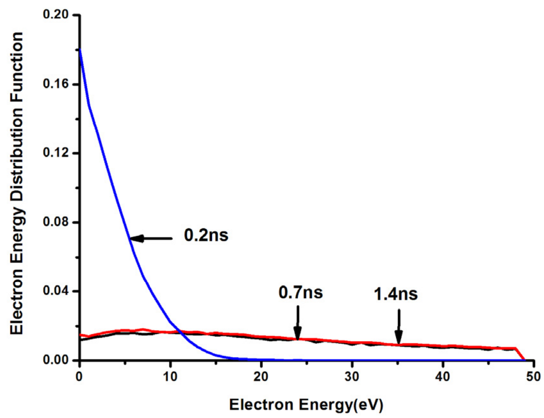

Fig. 5. The electron energy distribution functions at the moment 0.2ns, 0.7ns and 1.4ns. Metal vapor density: 10^{23} m^{-3}; Voltage: 5kV

Fig. 6 shows the influence of neutral metal vapor on the process of electron avalanche. The applied voltage was 10kV. The starting time of the electron avalanche increased from 0.2ns to 0.4ns as the neutral metal vapor density increased from 10^{21} m^{-3} to 10^{23} m^{-3}. The curve for metal vapor density 10^{23} m^{-3} is higher than the curve for density 10^{22} m^{-3}, but the difference is slight. However, the curve for metal vapor density 10^{21} m^{-3} is much lower than the two curves. The results indicate that a higher neutral metal vapor density can accelerate the electron avalanche process but the influence was restricted when the density exceeded a certain level.

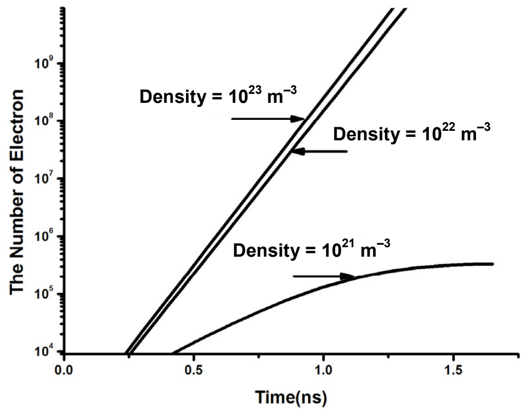

Fig. 6. The influence of neutral metal vapor density on the processes of electron avalanche. The applied voltage: 10kV.

Fig. 7 shows the boundary of instantaneous breakdown region. The breakdown boundary decreased with the metal vapor density increased. When the metal vapor density exceeded a certain level 10^{21} m^{-3}, a breakdown occurred in case the applied voltage exceeded 1kV. For a low pressure discharge, the density of metal vapor may be a critical factor that determines the instantaneous breakdown boundary of a VCB.

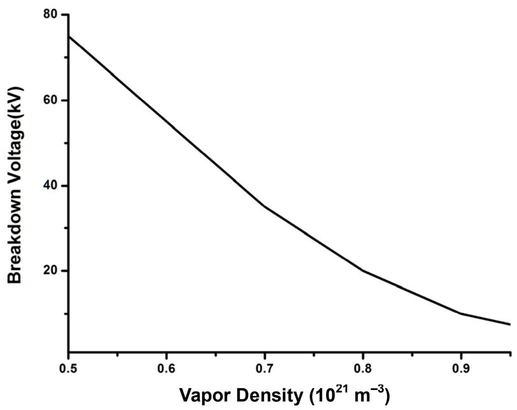

Fig. 7. The minimum breakdown voltages for different neutral vapor densities.

III. CONCLUSIONS

We adopted a PIC-MCC method to simulate breakdowns in copper vapor at a density of interruption limit. A model with one dimension in physical space and three dimensions in velocity space was developed. The model considered ionization, excitation, elastic collision and secondary emission. We obtained the boundary of instantaneous breakdown region through the simulation. The results show that a higher neutral metal vapor density can accelerate the electron avalanche process but the influence was limited when the density exceeded a threshold. Moreover, a higher voltage can also accelerate the avalanche process.

REFERENCES

[1] E. Dullni, E. Schade, and B. Gellert, "Dielectric Recovery of Vacuum Arcs after Strong Anode Spot Activity," IEEE Trans. Plasma Sci., vol. 15, pp. 538-544, Oct 1987.

[2] E. Schade and E. Dullni, "Recovery of breakdown strength of a vacuum interrupter after extinction of high currents," IEEE Trans. Dielectr. Electr. Insul., vol. 9, pp. 207-215, Apr 2002.

[3] S. W. Rowe, "The Intrinsic Limits of Vacuum Interruption," Isdeiv 2008: Proceedings of the Xxiiird International Symposium on Discharges and Electrical Insulation in Vacuum, Vols 1 and 2, pp. 192-197, 2008.

[4] E. Dullni and E. Schade, "Investigation of High-Current Interruption of Vacuum Circuit-Breakers," IEEE Trans. Electr. Insul., vol. 28, pp. 607-620, Aug 1993.

[5] S. Yanabu, E. Kaneko, T. Tamagawa, K. Matsumoto, and M. Homma, "Post-Arc Current after High-Current Interruption in Vacuum," IEEE Trans. Electr. Insul., vol. 20, pp. 739-744, 1985.

[6] R. Holmes and S. Yanabu, "Post-Arc Current Mechanism in Vacuum Interrupters," Journal of Physics D-Applied Physics, vol. 6, pp. 1217-1231, 1973.

[7] G. Duning and M. Lindmayer, "Plasma density decay of vacuum discharges after current zero," IEEE Trans. Plasma Sci., vol. 27, pp. 923-929, Aug 1999.

[8] J. G. Andrews and R. H. Varey, "Sheath Growth in a Low Pressure Plasma," Phys.Fluids, vol. 14, pp. 339-343, 1971.

[9] P. Sarrailh, L. Garrigues, G. J. M. Hagelaar, G. Sandolache, S. Rowe, B. Jusselin, and J. P. Boeuf, "Expanding sheath in a bounded plasma in the context of the post-arc phase of a vacuum arc," J. Phys. D: Appl. Phys., vol. 41, p. 015203, Jan 7 2008.

[10] C. K. Birdsall, "Particle-in-Cell Charged-Particle Simulations, Plus Monte-Carlo Collisions with Neutral Atoms, Pic-Mcc," IEEE Trans. Plasma Sci., vol. 19, pp. 65-85, Apr 1991.

[11] V. Vahedi and M. Surendra, "A Monte-Carlo Collision Model for the Particle-in-Cell Method - Applications to Argon and Oxygen Discharges," Comput. Phys. Commun., vol. 87, pp. 179-198, May 1995.

[12] M. A. Furman and M. T. F. Pivi, "Probabilistic model for the simulation of secondary electron emission," Phys. Rev. S. Accel. Beams, vol. 5, p. 124404, 2002.

E-mail of the author: liuzy@mail.xjtu.edu.cn

philowzx@gmail.com